# A Multiple Model Based Approach for Deep Space Power **System Fault Diagnosis**

Marc A. Carbone<sup>1</sup>, Jeffrey T. Csank<sup>2</sup>, Brian J. Tomko<sup>3</sup>, Jeffrey C. Follo<sup>4</sup>, Matthew J. Muscatello<sup>5</sup> NASA Glenn Research Center, Cleveland, OH, 44135, USA

Improving protection and health monitoring capabilities onboard the electrical power system (EPS) for spacecraft is essential for ensuring safe and reliable conditions for deep space human exploration. Electrical protection and control technologies on the National Aeronautics and Space Administration's (NASA's) current human space platform relies heavily on ground support to monitor and diagnose power systems and failures. As communication bandwidth diminishes for deep space applications, a transformation in system monitoring and control becomes necessary to maintain high reliability of electric power service. This paper presents a novel approach for on-line power system security monitoring of autonomous deep space spacecraft.

#### Nomenclature

**EPS** = Electrical Power System DST= Deep Space Transport

APC= Autonomous Power Controller FDI= Fault Detection and Isolation

FDIR = Fault Detection, Isolation, and Recovery

= Artificial Intelligence

= Sequential Probability Ratio Test **SPRT** = Multiple Model Adaptive Estimation MMAE**DERs** = Distributed Energy Resources **PMAD** = Power Management and Distribution

TPR= True Positive Rate = True Negative Rate TNR= False Positive Rate FPR= False Negative Rate **FNR** 

### I. Introduction

NASA is investing heavily in autonomy for deep space vehicles and aeronautics applications. These autonomous power systems have the ability to control and are activities. power systems have the ability to control and reconfigure a power system for changing conditions such as faults. The ability to detect and diagnose faults in complex processes is one of the most important functions of an autonomous system. An example of this type of application is the electrical power system (EPS) of a deep space vehicle, such as the deep space transport (DST) which is destined to travel to Mars by the 2030s. The early observation of incipient faults may prevent power system failures, and widespread blackouts that could result in catastrophic damage to other subsystems and even risk human lives. Currently, human rated spacecraft power systems rely on human operators to diagnose faults by carefully examining acquired telemetry. As NASA moves towards deep space exploration, the distance from earth at which these spacecraft operate increases greatly. This distance increases the time it takes to receive telemetry from the spacecraft, resulting in longer times to recover and reconfigure after a fault. Without the constant monitoring and analysis from the ground, the EPS is at risk of faults going undetected by circuit breakers or

<sup>&</sup>lt;sup>1</sup> Electrical Engineer, Power Management and Distribution Branch, marc.a.carbone@nasa.gov, Non-Member

<sup>&</sup>lt;sup>2</sup> Electrical Engineer, Power Management and Distribution Branch, jeffrey.t.csank@nasa.gov, AIAA Sr. Member

<sup>&</sup>lt;sup>3</sup> Computer Scientist, Scientific Applications Branch, brian.j.tomko@nasa.gov, Non-Member

<sup>&</sup>lt;sup>4</sup> Computer Engineer, Flight Software Branch, jeffrey.c.follo@nasa.gov, Non-Member

<sup>&</sup>lt;sup>5</sup> Computer Engineer, Flight Software Branch, matthew.j.muscatello@nasa.gov, Non-Member

faults persisting in the system in the event of a failure in hardware protection. Therefore on-board failure monitoring capabilities for these types of power systems are critical for mission success.

This work extends on prior efforts in the development of an autonomous power controller (APC) for deep space vehicles.<sup>1,2</sup> The APC is responsible for safely operating and protecting the electrical power system, which includes managing the energy and power usage by the loads, and fault management.<sup>3</sup> This paper will describe some of the ongoing development of a fault management system for a deep space exploration spacecraft autonomous power controller.

#### II. Power-Related Fault Overview

DC power systems are susceptible to a variety of fault types that can potentially cause partial or total loss of the system loads. A fault can be defined as an unpermitted deviation of at least one characteristic property or parameter of the system from the acceptable, usual, or standard condition.<sup>4</sup> Fault is used as general term that encompasses a wide variety of problems that can arise in a power system including failures and malfunctions. Several efforts in power system fault management have focused largely on individual power system components, such as inverters, generators, batteries, and relays. In addition, much of the research has considered only AC systems. This study will consider a DC power system consisting of electronic loads, solar arrays, battery storage, and switching components, with current and voltage measurements available throughout. Some of the fault types may include stuck switches, open circuits, solar array and battery faults, and communication failures, amongst others. Many fault types are able to be protected locally using circuit breakers, relays, and other physical protective devices. Certain events such as high impedance short circuits and sensor failures require data from beyond the immediate location of the event to diagnose, and therefore must be analyzed using system-wide information. This paper will provide a method for detecting and diagnosing high impedance short circuits and sensor failures on a deep space vehicle power system.

## A. Power System High Impedance Fault

For the application of a spacecraft DC power system there are several fault types that can cause loss of power to the system or physically damage system equipment. Therefore the protection and control schemes of these types of power systems are critically important for mission success. In general, the most common power system fault is the short circuit. This is commonly addressed using current measuring circuit breakers and reclosers to detect a rapid increase in current in order to activate the breaker. If a short circuit is allowed to persist, power system components can be damaged or destroyed due to the high flow of current. Therefore, it is critical to the safety of the power system for the short to be detected and isolated from the rest of the circuit as soon as possible. This may result in losing the ability to power certain loads until the cause of the short is fully isolated. The best case protection design will be to isolate the short circuit while disabling the fewest loads. In order to do this the power system control must monitor for short circuits at all times.

Short circuits can be categorized into two main types, hard and soft short circuits. Hard short circuits take place when a direct short circuit makes contact to ground. These faults draw high amounts of current that can cause cascading damage if not isolated quickly. This is largely due to the rapid increase in heat that results from the fault current. According to Gonzalez et. al. is it is normally desirable to isolate hard shorts in 0.25 to 0.5 seconds, or sooner if possible. Traditionally, local hardware protection is included to handle these types of faults. These types of circuit breakers rely on an internal trip signal that trips nearly instantaneously for hard shorts, and for lower level faults, they trip on  $(i^2t)$  or under voltage. Thus hard faults, while more common, are relatively easy to detect and isolate.

Conversely, soft short circuits, commonly referred to as soft faults, can be much more difficult to detect and isolate. In the event of a soft short circuit, there is a resistance between the shorted line and ground, thus limiting the fault current. These types of faults tend to have less damaging effects, however, they can lead to a hard short, so it is still important to detect and isolate them quickly. The level of the fault current is often too low to use normal limit checking circuit protection. The fault current will potentially be indistinguishable from the normal operating current causing many false trips in the system or no trip when there is actually a soft fault. Over tripping would result in poor performance of the distribution system in that it may interrupt service to many loads. Therefore the case of the soft short circuit becomes very difficult to diagnose at the local level. Thus more system information is needed to detect and isolate these types of faults. One solution is to use a central controller to monitor the global system variables, using a system model.

#### **B.** Sensor Faults

Sensor monitoring and validation is a crucial aspect in determining the fault status of the power system. Because current and voltage sensors are subjected to white Gaussian noise, diagnostic algorithms can become less accurate as

the signal to noise ratio increases. Terrestrial power systems rely on the concept of state estimation to reduce the effects of sensor noise and to generate data at locations where sensor readings may not be available. The Kalman filtering method described in section IV can be used to provide optimal state estimates for the noisy power system sensors. Statistical testing can be used to isolate sensor faults, in the event that a sensor becomes biased, excessively noisy, or stuck. These types of sensor failures would go unnoticed or set off false alarms under less sophisticated model-free approaches, therefore it is critical to identify these types of faults in the network.

## III. Model-Based Fault Detection, Isolation, and Reconfiguration

Fault detection isolation, and reconfiguration (FDIR) is a critical component of system resiliency, in particular for creating more intelligent and autonomous power systems. FDIR ensures continual safe and acceptable operation of a system when a fault occurs. The performance of a fault diagnostic controller can be characterized by its *fault sensitivity*, *reaction speed*, and *robustness*. Fault sensitivity is the controller's ability to detect faults of a reasonably small size; reaction speed defines the ability of the controller to detect and isolate faults with minimal delay; and robustness is the ability of the controller to operate in the presence of noise, and disturbances with few false alarms.<sup>6</sup> These benchmarks offer a quantifiable measure of the performance of the method.

An important concept of FDIR frequently used is analytical redundancy. Analytical redundancy can be divided into two main categories, qualitative and quantitative. Intuitively, the quantitative based methods use models derived directly from mathematical equations to generate residuals for fault detection and isolation, whereas the qualitative based methods rely on other techniques such as artificial intelligence (AI) and pattern recognition to capture differences between predicted and actual behavior.

In general, quantitative model-based methods take place in three steps. The first step is to generate a set of residuals. Using the concept of analytical redundancy, we may define a residual as the difference between a measured output and an estimated output,

$$r(t) = y(t) - \hat{y}(t). \tag{1}$$

The residuals in a fault detection scheme should satisfy two properties,

- 1. Invariance Relation: When no fault occurs, the mean of the residual should be zero. E[r(t)] = 0
- 2. Fault Detectability: When any of the faults in the model occur, the residual E[r(t)] should deviate from zero.

Ideally, the residuals should be insensitive to noise, disturbances, and model uncertainties. Therefore it is important for a fault diagnostic controller to generate robust residuals which are insensitive to unwanted corruption, but sensitive to only real system faults.

The second step in model-based fault detection and diagnosis is to make the decision of whether a fault has occurred (detection) and the location and type of fault (isolation) based on the residual signature. There are several existing techniques for detection and isolation of faults using the residuals. The final action is for the controller to perform an online reconfiguration in response to any detected fault(s). Fault detection and diagnostic controllers using model based methods include fault detection filters, observer-based methods, parameter estimation methods, and parity relation methods to name a few.

## IV. Kalman Filter-Based Approach

The Kalman filter-based approach uses its innovation sequence to generate residuals for FDI, as introduced by Mehra and Peschon<sup>7</sup> in 1971. The decision making process for the Kalman filter is done through statistical testing on whiteness, mean, and covariance of the residuals. The most common tool for these tests is the Maximum Likelihood Ratio. The whiteness and unit variance properties of the Kalman filter residuals allows us to easily validate sensor data and diagnose changes in sensor noise, and stuck sensors, which will be demonstrated in Section V.

An important development in Kalman filter-based FDI is the multiple model adaptive estimation (MMAE) approach.<sup>8</sup> Here we use a linear stochastic system model with uncertain parameters to represent the faults in the state matrices. With this framework, we can design a Kalman filter for each fault scenario, resulting in a bank of Kalman

filters to use for fault detection and isolation. The MMAE approach has been implemented on several aerospace applications including aircraft flight control and internal navigation systems. An attractive feature of this technique is that since the number of fault modes is finite, the control designer can create a fault model corresponding to each unique type. However, as the amount of fault types becomes larger, the computational costs increase as well. One solution to this is to run the fault models in parallel independently. For certain system failure types, the fault parameter changes as the component or subsystem fails. A realistic approach to this problem is the Interacting Multiple Model Approach developed by Zhang and Li.<sup>9</sup> In this approach a failure is modeled as a finite Markov chain with known transition probabilities. The algorithm adjusts the Kalman filter parameters based on Gaussian approximations and hypothesis merging, otherwise known as "mixing".

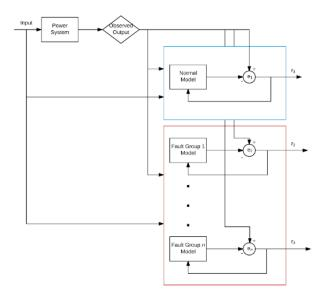


Figure 1. Block diagram of the multiple model Kalman filter-based diagnostic algorithm.

## A. Algorithm for Fault Diagnostics

Expanding upon the work of Wiener<sup>10</sup>, R.E. Kalman developed a solution to the common filtering and prediction problem for dynamic systems.<sup>11</sup> We will discuss the Kalman filter algorithm and a few of the statistical properties of the Kalman filter's innovations sequence which will be used for fault diagnosis. We are able to define the Kaman filter algorithm based on Mehra and Peshon's framework. First we will consider a discrete-time linear dynamic system model.

$$x_{i+1} = \boldsymbol{\Phi}_i x_i + \boldsymbol{G}_i u_i + \boldsymbol{\Gamma}_i w_i \tag{2}$$

$$z_i = \mathbf{H}_i x_i + \nu_i \tag{3}$$

Where

- $x_i$  is the  $n \times 1$  vector of the state variables
- $u_i$  is the  $p \times 1$  vector of the control variables
- $w_i$  is the  $q \times 1$  vector of random forcing functions
- $z_i$  is the  $r \times 1$  vector of the output variables (observables)
- $v_i$  is the  $r \times 1$  vector of random measurement errors
- $\Phi_i$  is the  $n \times n$  state transition matrix
- $G_i$  is the  $n \times p$  input distribution matrix
- $\Gamma_i$  is the  $n \times q$  noise distribution matrix

## • $H_i$ is the $r \times n$ output matrix

the subscript i denotes the time instant, and characters in bold are matrices. Note that the random vectors  $w_i$  and  $v_i$  are Gaussian and white. This will be useful for statistical testing later on. Next we may define our innovation sequence as:

$$v_i = z_i - \hat{z}_{i/i-1} \tag{4}$$

where  $\hat{z}_{i/i-1}$  denotes the unbiased minimum variance estimate of  $z_i$  based on the observed measurements up to time (i-1). Using the Kalman filter algorithm, we are able to generate the innovation sequence.

$$\bar{x}_{i+1/i} = \boldsymbol{\Phi}[\bar{x}_i + \boldsymbol{K}_i v_i] + \boldsymbol{G}_i u_i + \boldsymbol{\Gamma}_i \overline{w}_i \tag{5}$$

$$\hat{x}_{o|-1} = x_0 \tag{6}$$

$$v_i = z_i - \mathbf{H}_i \hat{x}_{i/i-1} - \bar{v}_i \tag{7}$$

$$K_{i} = P_{i/i-1} H_{i}^{T} (H_{i} P_{i/-1} H_{i}^{T} + R_{i})^{-1}$$
(8)

$$\mathbf{P}_{i+1/i} = \mathbf{\Phi}_i \mathbf{P}_i \mathbf{\Phi}_i^T + \mathbf{\Gamma}_i Q_i \mathbf{\Gamma}_i^T \tag{9}$$

$$\mathbf{P}_{i/i} = (I - \mathbf{K}_i \mathbf{H}_i) \mathbf{P}_{i/i-1} \tag{10}$$

Here  $\hat{x}_{i/j}$  is the unbiased minimum variance estimate of  $x_i$  based on observations up to time j.

- $K_i$  is the  $n \times r$  Kalman gain matrix
- $P_{i/i}$  is the error covariance of  $\hat{x}_{i/j}$

In order to test the Kalman Filter algorithm we must ensure that the innovation sequence is white, thus independent at different time instants. To test that our statistical assumptions are true over a sampled distribution, we create a test of significance. Using this test we are able to determine how closely the sample distribution matches our hypothesis. Under the null hypothesis the autocorrelation function  $c_k$  for k = 1, 2, ... are asymptotically independent with zero mean and covariance l/N, where N is the number of samples. They can be treated as samples from the same normal distribution and must lie within the range of  $1.96/\sqrt{N}$  more than 95 percent of the time to validate the null hypothesis. To do this we must test that the sequence is both zero mean and uncorrelated (i.e. zero covariance). Below we define how to calculate the standardized innovation sequence as well as the discrete estimates for mean and covariance.

$$\eta_i = (H_i P_{i/i-1} H_i^T + R_i)^{-\frac{1}{2}} v_i \tag{11}$$

Using this we can calculate the mean of the sample mean of the standardized innovation sequence

$$\hat{\bar{\eta}} = \frac{1}{N} \sum_{i=1}^{N} \eta_i \tag{12}$$

where N is the number of samples, and  $\bar{\eta}$  is the true mean of the innovation sequence. To test this under the null hypothesis,  $\bar{\eta}$  has a Gaussian distribution with zero mean and covariance. Thus 95 percent of the time we expect

$$|\hat{\eta}| > 1.96 I/\sqrt{N}$$
 (13)

for the null hypothesis to hold true. Secondly, we must show that the innovation sequence is uncorrelated (i.e. covariance equal to zero). We can estimate this as,

$$\hat{c}_o = \frac{1}{N} \sum_{i=1}^{N} (\eta_i - \hat{\eta}) (\eta_i - \hat{\eta})^T$$
 (14)

Using the Kalman filter-based fault diagnosis method, the application of power system faults for space vehicles is examined.

## V. Implementation and Simulation Results

The main objective of this study is to develop a model-based FDI algorithm, capable of detecting and isolating faults at the central level of the APC. The data used to test the fault management scheme was created in MATLAB®/Simulink® (the Math Works, Inc.) by PC Krause and Associates to model a simplified version of the DSG using models of NASA's Power Management and Distribution (PMAD) power electronics. We will test the feasibility of the controller by its ability to correctly detect and isolate a variety of power system fault scenarios. The test network is shown below in Figure 2. The configuration includes generation from solar arrays with dc regulators (SA 1, 2) and battery storage units which also have charge and discharge regulation (BATT 1, 2). In the middle of the network there are main bus switching units (Bus 3 and 7), and further downstream (to the right) are power distribution units (Bus 4 and 8), responsible for providing energy to the constant power loads.

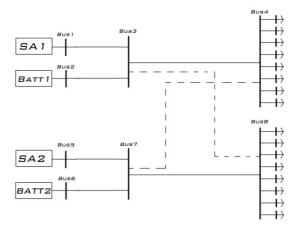


Figure 2. One-line diagram of the test power system.

To model the power distribution system we use develop connectivity matrix using DC nodal analysis. In this scheme, our state vector  $\mathbf{x}$  consists of all the bus voltages in the network. To populate the current measurements in this matrix for any power system, two rules apply:

Diagonal Elements: 
$$Y_{kk} = sum \ of \ the \ add mittances \ connected \ to \ bus \ k$$
 (15)

Off-diagonal Elements: 
$$Y_{kn} = -(sum \ of \ add mittances \ between \ bus \ k \ and \ n)$$
 (16)

Where  $Y_{kn}$  is the admittance of the line between bus k and n. The connectivity matrix can be used to relate bus voltages and line currents everywhere in the power system. Naturally, this will be a useful tool to model different types of faults in our global controller scheme. For the upper string of Figure 2, our nodal DC analysis for voltages and currents is,

$$\begin{bmatrix} I_{13} \\ I_{23} \\ 0 \\ I_{34} \end{bmatrix} = \begin{bmatrix} Y_{13} & 0 & -Y_{13} & 0 \\ 0 & Y_{23} & -Y_{23} & 0 \\ -Y_{13} & -Y_{23} & Y_{13} + Y_{23} + Y_{34} & -Y_{34} \\ 0 & 0 & -Y_{34} & Y_{34} \end{bmatrix} \begin{bmatrix} V_1 \\ V_2 \\ V_3 \\ V_4 \end{bmatrix}$$
(17)

We can expand on this framework to include current for each switch in the network, output voltages for solar array and battery busses, as well as input and output voltages for Bus 3, 4, 7, and 8 switches. In addition, we can remove row 6 above because it represents the net current injected into Bus 3, which is always equal to zero because it is a distribution bus. Using these equations we can create a model for the observed currents and voltages in the normal operating power system of Figure 2.

In order to model a short circuit on one of the lines we can manipulate the connectivity matrix to account for current leakage on one of the lines. Using this methodology we are able to model a short circuit of any resistance regardless of the power output level. Sensor faults are also able to be isolated using the standardized innovation sequence of the Kalman filter. Sensor fault isolation will be discussed in greater detail below.

#### A. Simulation Results

To demonstrate the effectiveness of the fault management design, we will run the simulation over several hundreds of test cases with varying fault parameters. We will run 100 cases for each fault type as well as well as 100 cases with no faults. Our fault types will include faults that require diagnosis at the central level, which include high impedance faults on all of the distribution lines and sensor biases on all of the network sensors ( $V_{out}$ ,  $V_{in}$ , I). For each fault case we vary the load level, eclipse state, and fault parameter. Fault parameters are sensor offset value, and short to ground impedance. An example of the controller running in the normal mode is displayed below in Figure 3.

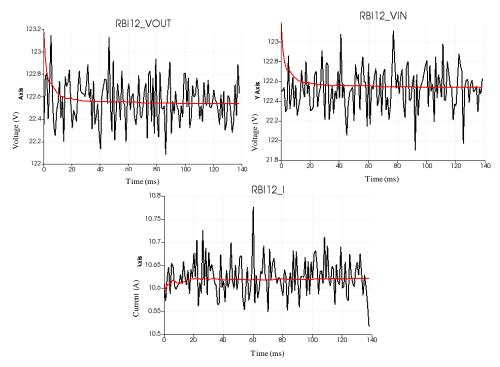


Figure 3. Voltage in, out, and current for a single RBI switch under normal operating conditions.

During the normal mode operation we can see that our Kalman filter gives us an optimal estimate (red) for the observed noisy sensor data (black), thus giving us a more trustworthy representation of the data to analyze. For spacecraft that may be in flight for several decades, the signal to noise ratio is liable to increase, therefore making optimal state estimation an important part of power system health monitoring. Our residuals are calculated by the innovation sequence of our normal mode filter, which consists of the difference between the observed data and the estimated data. The fault diagnostic algorithm runs the tests for whiteness, mean, and covariance to diagnose faults in the system.

When a fault in the system occurs, the residual sequence of the normal model fails one or more of the statistical tests, and the fault models are launched in parallel. If one of the fault model filters is able to pass the tests for white ness, mean, and covariance, then the controller is able to successfully isolate the type of fault. The example in Figure 4 shows a high impedance fault on the line in between Bus 2 and Bus 3. The current leakage to ground breaks the normal model filter, and the fault models are subsequently launched. The controller is able to correctly identify the fault as a high impedance short on the correct line, by matching the model with the particular fault to the incoming residual window. Using all of the state estimates of the power system, we are able to confidently isolate the fault, and prevent false alarms by minimizing noise and relying on multiple system variables to make the diagnosis.

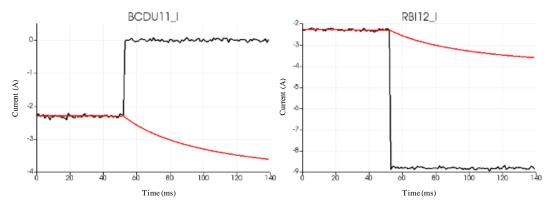


Figure 4. High impedance short to ground fault between Bus2 and Bus3

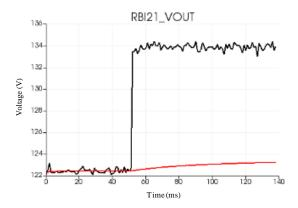


Figure 5. Sensor offset on a Bus7 voltage sensor.

Another test we will demonstrate is a sensor offset. In this scenario, a sensor may deviate from its true value, which may cause problems in the analysis of other power system algorithms. Therefore it is critical to isolate a sensor fault from a fault in the hardware. Figure 5 shows the normal model estimates for a biased sensor on an input voltage to Bus5 (RBI2-1\_Vout). Again the residual sequence of the controller in the normal mode fails the statistical tests described above. Then the code determines the sensor with the largest residual and autonomously generates a filter model with the suspected sensor removed. Finally, the controller is able to isolate the sensor fault by matching the data to the new sensor fault filter. This general process is common for performing power system state estimation and sensor validation on terrestrial power systems. One advantage of the Kalman filter approach is that the controller analyses the residuals over a window of time and determines the result based on the mean of the innovation sequence. This means that this method will be more robust in the face of transients and occasional out-of-sync data. More basic techniques only rely on instantaneous data, which can lead to problems in the event of data mismatches, disturbances, and transients.

The main challenge in isolating a large number of fault types with limited data observability is differentiating between indistinguishable fault types. In this case the output data for some of the high impedance short circuits looks

identical to a current sensor offset. One potential solution to this may be the addition of power system testing. In such a situation, a set of certain allowable actions may be taken (such as opening a switch or turning off a device) in order to collect additional data and isolate the fault type. This is an area for future work in this field known as active fault diagnosis.

To summarize the results thus far, a confusion matrix has been developed to determine at what rate the controller was able to correctly diagnose the inserted fault. 2,800 fault and non-fault scenarios were generated in total for this study. The classification results for all of the faults inserted on one string of the power system can be seen in Table II of Appendix A. When a fault was inserted in the simulation, the condition is considered positive. If the controller was able to correctly diagnose the fault, then the predicted condition is also found to be positive. For a non-faulted simulation, the condition is negative; likewise when no fault is found by the controller the predicted condition is negative. The confusion matrix consists of four elements, True Positive Rate (TPR), True Negative Rate (TNR), False Positive Rate (FPR), and False Negative Rate (FNR). They are calculated by the following equations with results presented in Table I.

$$TPR = \frac{\sum predicted\ condition\ positive}{\sum\ condition\ positive}$$
(18)

$$TNR = \frac{\sum predicted\ condition\ negative}{\sum condition\ negative}$$
(19)

$$FPR = \frac{\sum predicted\ condition\ positive}{\sum\ condition\ negative}$$
 (20)

$$FNR = \frac{\sum predicted\ condition\ negative}{\sum\ condition\ positive}$$
 (21)

**Table I. Confusion Matrix for DC Power System Faults** 

|                | Predicted Condition |          |
|----------------|---------------------|----------|
| True Condition | TPR: 87%            | FPR: 1%  |
|                | FNR: 1.89%          | TNR: 99% |

#### VI. Conclusion

Autonomous power systems must have the ability to detect, isolate, and recover from power system failures. This paper proposed using a Kalman filter approach to perform fault management to detect short circuits and sensors failure within a space DC microgrid. By analyzing a sequence of time series residuals we are able to isolate faults (such as a stuck sensor) that less robust model-free methods cannot. In addition, residual sequence analysis gives our FDI method improved robustness in the face of transients and other disturbances, unlike simpler methods. The challenge of isolating high impedance short circuits as well as various sensor failures was identified for space power applications, and therefore was a suitable first candidate for our FDI technique. Lastly, we show the simulation results for a small DC system with simulated PMAD components. Overall the method was shown to be successful in detecting and isolating high and low impedance short circuits and sensor failures.

## Appendix A

Table II. Classification Results for a Single String of Simulation Faults

|           | Predicted Condition |       |       |       |       |       |       |       |       |       |          |          |          |          |          |          |
|-----------|---------------------|-------|-------|-------|-------|-------|-------|-------|-------|-------|----------|----------|----------|----------|----------|----------|
|           |                     | $f_I$ | $f_2$ | $f_3$ | $f_4$ | $f_5$ | $f_6$ | $f_7$ | $f_8$ | $f_9$ | $f_{10}$ | $f_{II}$ | $f_{12}$ | $f_{13}$ | $f_{14}$ | $f_{15}$ |
| True      | $f_{l}$             | 71    | 0     | 0     | 0     | 0     | 0     | 0     | 0     | 6     | 0        | 0        | 0        | 0        | 0        | 0        |
| Condition | $f_2$               | 0     | 100   | 0     | 0     | 0     | 0     | 0     | 0     | 0     | 0        | 0        | 0        | 0        | 0        | 0        |
|           | $f_3$               | 0     | 0     | 98    | 2     | 0     | 0     | 0     | 0     | 0     | 0        | 0        | 0        | 0        | 0        | 0        |
|           | $f_4$               | 0     | 0     | 0     | 99    | 0     | 0     | 0     | 0     | 0     | 0        | 0        | 0        | 0        | 0        | 0        |
|           | $f_5$               | 0     | 1     | 0     | 8     | 65    | 0     | 0     | 0     | 0     | 0        | 0        | 0        | 0        | 22       | 0        |
|           | $f_6$               | 0     | 0     | 0     | 0     | 0     | 100   | 0     | 0     | 0     | 0        | 0        | 0        | 0        | 0        | 0        |
|           | $f_7$               | 0     | 0     | 0     | 0     | 0     | 0     | 100   | 0     | 0     | 0        | 0        | 0        | 0        | 0        | 0        |
|           | $f_8$               | 0     | 0     | 0     | 17    | 0     | 0     | 0     | 83    | 0     | 0        | 0        | 0        | 0        | 0        | 0        |
|           | $f_9$               | 0     | 0     | 0     | 0     | 0     | 0     | 0     | 0     | 100   | 0        | 0        | 0        | 0        | 0        | 0        |
|           | $f_{10}$            | 0     | 0     | 0     | 1     | 0     | 0     | 0     | 0     | 0     | 98       | 0        | 0        | 0        | 0        | 0        |
|           | $f_{II}$            | 0     | 1     | 19    | 0     | 0     | 0     | 0     | 0     | 0     | 0        | 80       | 0        | 0        | 0        | 0        |
|           | $f_{l}$             | 0     | 0     | 0     | 0     | 0     | 0     | 0     | 0     | 0     | 0        | 0        | 100      | 0        | 0        | 0        |
|           | $f_{13}$            | 0     | 0     | 0     | 0     | 0     | 0     | 0     | 0     | 0     | 0        | 0        | 0        | 100      | 0        | 0        |
|           | $f_{14}$            | 0     | 0     | 0     | 2     | 5     | 0     | 0     | 0     | 0     | 0        | 0        | 0        | 0        | 83       | 0        |
|           | $f_{15}$            | 0     | 0     | 0     | 0     | 0     | 0     | 0     | 0     | 0     | 0        | 0        | 0        | 0        | 9        | 91       |

**Table III. Fault Descriptions for Simulation Testing** 

| Fault Name | Description                              |
|------------|--|
| $f_I$      | Bus6-Bus7 High Impedance Short-to-Ground |
| $f_2$      | BCDU2 Vout Sensor Offset                 |
| $f_3$      | Bus7-Bus8 High Impedance Short-to-Ground |
| $f_4$      | No Fault                                 |
| $f_5$      | RBI2-1 I Sensor Offset                   |
| $f_6$      | RBI2-1 V <sub>in</sub> Sensor Offset     |
| $f_7$      | RBI2-1 V <sub>out</sub> Sensor Offset    |
| $f_8$      | RBI2-2 I Sensor Offset                   |
| $f_9$      | RBI2-2 V <sub>in</sub> Sensor Offset     |
| $f_{IO}$   | RBI2-2 V <sub>out</sub> Sensor Offset    |
| $f_{II}$   | RBI2-4 I Sensor Offset                   |
| $f_{12}$   | RBI2-4 V <sub>in</sub> Sensor Offset     |
| $f_{13}$   | RBI2-4 V <sub>out</sub> Sensor Offset    |
| $f_{14}$   | Bus5-Bus7 High Impedance Short-to-Ground |
| $f_{15}$   | SSU2 V <sub>out</sub> Sensor Offset      |

## Acknowledgements

The authors would like to thank Advanced Exploration Systems Project, AES Chief Technologist James Soeder, AMPS Project Manager Karin Bozak, Long Truong, Yu Hin (Billy) Hau, PC Krause and Associates, and Dr. Kenneth Loparo for their support in this work.

#### References

<sup>&</sup>lt;sup>1</sup> May, R.D., et. al. "An Architecture to Enable Autonomous Control of Spacecraft," AIAA-2014-3834, AIAA Propulsion and Energy Forum, 12<sup>th</sup> International Energy Conversion Engineering Conference, Cleveland, OH, July 28-30, 2014.

<sup>&</sup>lt;sup>2</sup> Dever, T.P., Trase, L.M., Soeder, J.F., "Application of Autonomous Spacecraft Power Control Technology to Terrestrial Microgrids," AIAA-2014-3836, AIAA Propulsion and Energy Forum, 12<sup>th</sup> International Energy Conversion Engineering Conference, Cleveland, OH, July 28-30, 2014.

- <sup>3</sup> Csank, J.T., et. al. "An Autonomous Power Controller for the NASA Human Deep Space Gateway," AIAA-2014-3834, AIAA Propulsion and Energy Forum, to be presented at the AIAA Propulsion and Energy Forum and Exposition, Cincinnati, OH, July 9-11, 2018.
- <sup>4</sup> Hwang, I., Kim S., Kim Y., and Seah, C. E., "A Survey of Fault Detection, Isolation, and Reconfiguration Methods," *IEEE Transactions on Control Systems Technology*, Vol. 18, 2010, pp. 636-653.
- <sup>5</sup> Gonzalez, A. J., et. al. "Model-Based, Real-Time Control of Electrical Power Systems," *IEEE Transactions on Systems, and Cybernetics*, Vol. 26. 1996, pp. 470-482.
- <sup>6</sup> Gertler, J., Fault Detection and Diagnosis in Engineering Systems. Vol. 1, New York, NY: Marcel Dekker, Inc., 1998.
- <sup>7</sup> Mehra, R. K., and Peschon J., "An Innovations Approach to Fault Detection and Diagnosis in Dynamic Systems," *Automatica*, Vol. 4, 1971, pp. 637-640.
- <sup>8</sup> Magill, D. T., "Optimal Adaptive Estimation of Sampled Stochastic Processes," *IEEE Trans. Aut. Control*, Vol. 10. 1965, pp. 434-439.
- <sup>9</sup> Zhang Y. M., and Li, X. R., "Detection and Diagnosis of Sensor and Actuator Failures Using IMM Estimator," *IEEE Transactions on Aerospace and Electrical Systems*, Vol. 34, 1998, pp. 1293-1313.
- <sup>10</sup> Wiener, N., The Extrapolation, Interpolation and Smoothing of Stationary Time Series, John Wiley & Sons, Inc., New York, N.Y. 1949.
- <sup>11</sup> Kalman, R. E., "A New Approach to Linear Filtering and Prediction Problems," *Transactions of the ASME-Journal of Basic Engineering*, Vol. 82, 1960, pp. 35-45.
- <sup>12</sup> Jenkins, Gwilym, and Watts D., Spectral Analysis and Its Applications, Holden-Day Inc., San Francisco, 1968.
- <sup>13</sup> Ricks, B., W., Mengshoel, O. J., "Methods for Probabilistic Fault Diagnosis: An Electrical Power System Case Study," *Annual Conference of the Prognostics and Health Management Society*, 2009, San Diego, CA.